Brain Stimulation 13 (2020) 1323–1332

Contents lists available at ScienceDirect

Brain Stimulation

journal homepage: http://www.journals.elsevier.com/brain-stimulation

Differential effects of vagus nerve stimulation paradigms guide clinical development for Parkinson's disease

Ariana Q. Farrand [a], Ryan S. Verner [b], Ryan M. McGuire [b], Kristi L. Helke [c], Vanessa K. Hinson [d], Heather A. Boger [a, *]

[a] Department of Neuroscience and Center on Aging, Medical University of South Carolina, 173 Ashley Ave, BSB Suite 403, MSC 510, Charleston, SC, 29425, USA
[b] Neuromodulation Division of LivaNova, PLC, 100 Cyberonics Blvd, Houston, TX, 77058, USA
[c] Department of Comparative Medicine, 114 Doughty St, STB 648, MSC 777; Department of Pathology and Laboratory Medicine, 165 Ashley Ave, Children's Hospital 309, MSC 908, Medical University of South Carolina, Charleston, SC, 29425, USA
[d] Department of Neurology, Medical University of South Carolina, 96 Jonathan Lucas St, CSB 309, MSC 606, Charleston, SC, 29425, USA

ARTICLE INFO

Article history:
Received 21 February 2020
Received in revised form
15 June 2020
Accepted 30 June 2020
Available online 3 July 2020

Handling editor: Mark S. George, MD

Keywords:
Parkinson's disease
Vagus nerve stimulation
Nigrostriatal system
Dopamine
Locus coeruleus
Norepinephrine

ABSTRACT

Background: Vagus nerve stimulation (VNS) modifies brain rhythms in the locus coeruleus (LC) via the solitary nucleus. Degeneration of the LC in Parkinson's disease (PD) is an early catalyst of the spreading neurodegenerative process, suggesting that stimulating LC output with VNS has the potential to modify disease progression. We previously showed in a lesion PD model that VNS delivered twice daily reduced neuroinflammation and motor deficits, and attenuated tyrosine hydroxylase (TH)-positive cell loss.
Objective: The goal of this study was to characterize the differential effects of three clinically-relevant VNS paradigms in a PD lesion model.
Methods: Eleven days after DSP-4 (N-(2-chloroethyl)-N-ethyl-2-bromobenzylamine, noradrenergic lesion, administered systemically)/6-OHDA (6-hydroxydopamine, dopaminergic lesion, administered intrastriatally) rats were implanted with VNS devices, and received either low-frequency VNS, standard-frequency VNS, or high-frequency microburst VNS. After 10 days of treatment and behavioral assessment, rats were euthanized, right prefrontal cortex (PFC) was dissected for norepinephrine assessment, and the left striatum, bilateral substantia nigra (SN), and LC were sectioned for immunohistochemical detection of catecholamine neurons, α-synuclein, astrocytes, and microglia.
Results: At higher VNS frequencies, specifically microburst VNS, greater improvements occurred in motor function, attenuation of TH-positive cell loss in SN and LC, and norepinephrine concentration in the PFC. Additionally, higher VNS frequencies resulted in lower intrasomal α-synuclein accumulation and glial density in the SN.
Conclusions: These data indicate that higher stimulation frequencies provided the greatest attenuation of behavioral and pathological markers in this PD model, indicating therapeutic potential for these VNS paradigms.

Introduction

Vagus nerve stimulation (VNS) is thought to affect the central nervous system by modifying brain rhythms via the nucleus of the solitary tract (NTS) [1]. The NTS projects to the locus coeruleus (LC), and firing rates of noradrenergic (NE) neurons in the LC are increased relative to the duration of VNS [2,3]. This leads to elevated NE release in target regions and protection against neurotoxicity [4,5]. VNS also modifies inflammatory pathways, and therefore has potential to provide an effective treatment strategy for neurodegenerative diseases associated with neuroinflammation, such as Parkinson's disease (PD) [6].

Current treatment strategies for people with PD target symptoms rather than the source of neurodegeneration, do not halt disease progression, and often have intolerable side effects [7]. Thus, disease-modifying therapies have become a focus for

* Corresponding author. Medical University of South Carolina, 173 Ashley Avenue BSB Suite 403, MSC 510, Charleston, SC, 29425, USA.
E-mail address: boger@musc.edu (H.A. Boger).

https://doi.org/10.1016/j.brs.2020.06.078

preclinical PD research. The link between early degeneration of the LC in PD and the enhanced LC output with VNS through indirect projections from the vagus nerve to the LC via NTS suggest that VNS has the potential to slow disease progression for PD [8,9]. Our research group has shown that two daily sessions of VNS attenuate motor deficits as well as substantia nigra dopaminergic (SN-DA) and LC-NE cell loss and reduce neuroinflammation in a toxin-induced PD model [10]. These data combined with the overlap in rodent and human vagal nerve circuitry [11] suggest high translational value of rodent studies using VNS and great therapeutic potential of VNS for PD; however, the ideal stimulation paradigm for PD remains to be determined.

Low frequencies of VNS (1–10 Hz) have been investigated for treatment of autoimmune conditions including rheumatoid arthritis and inflammatory bowel disorders [12,13], as well as modulation of gut motility in animals [14]. Clinical work in rheumatoid arthritis indicates low VNS frequencies may be effective even when delivered as infrequently as one min per day [15]. While the mechanism of action for VNS in these autoimmune conditions remains unknown, some evidence suggests that modulation of

A

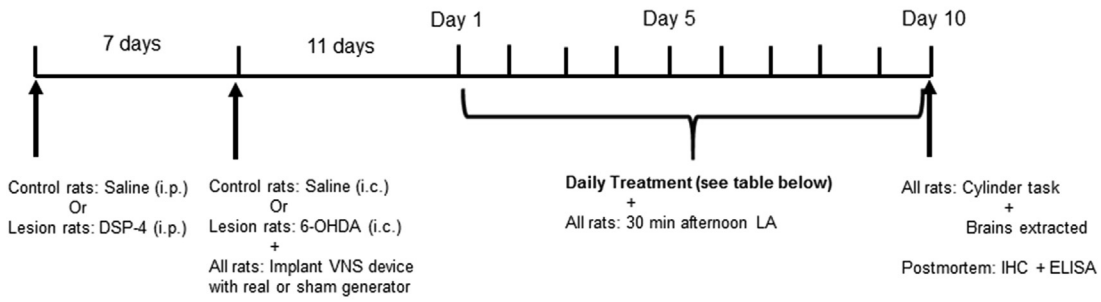

B

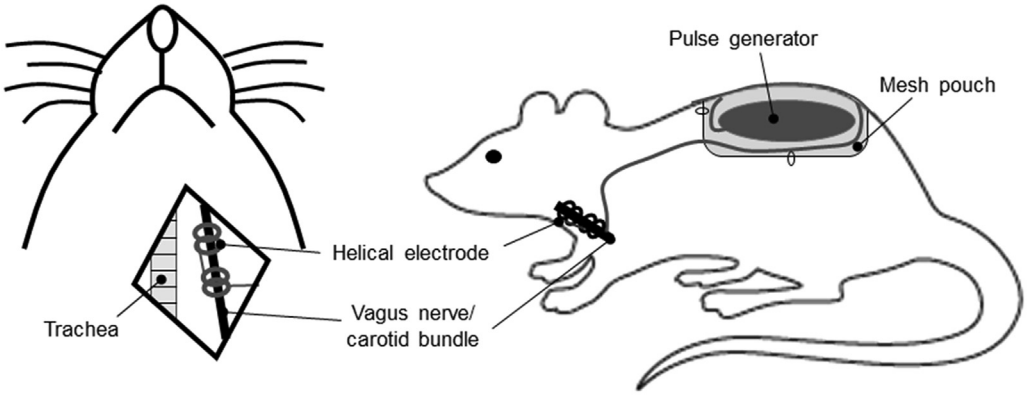

C

Parameters for treatment paradigms

Treatment Group	Dose	Pulse Width	Pulse Frequency	Dose Frequency/ Duration	Rationale
lowVNS	0.75 mA	250 μs	10 Hz	30 min on 23.5 hr off	Systemic anti-inflammatory standard
stdVNS	0.75 mA	250 μs	20 Hz	30 sec on 5 min off 24 hr/day	Epilepsy clinical standard
burstVNS	0.75 mA	250 μs	300 Hz 10 pulses per burst	19 sec interburst interval 24 hr/day	Biomimetic experimental therapy

Fig. 1. Experimental Design. (A) The PD-like lesion was implemented by administering DSP-4 (50 mg/kg, i.p.) followed by intrastriatal 6-OHDA (6 μg/μL, 2 μL/site) 7 days later. Control rats received saline injections. Next, either real or sham VNS stimulators were implanted. All rats then underwent 10 treatment days with daily locomotor activity (LA) assessment. The final treatment day, motor impairment was further assessed via the cylinder task. Rats were sacrificed and tissue processed for immunohistochemistry (IHC) and ELISA. (B) VNS implant diagram shows helical electrodes wrapped around the left vagus nerve and carotid artery bundle, with leads running subcutaneously to the pulse generator that was inserted into a mesh pouch and sutured to underlying back muscle. Diagram adapted from Ref. [76]. (C) Table details parameters of each treatment paradigm delivered for the specified group across the 10 treatment days.

systemic inflammatory pathways plays a role in the observed therapeutic effects [16].

Moderate stimulation frequencies (20–30 Hz) are common VNS parameters used for the treatment of epilepsy and depression. At these frequencies, intermittent stimulation activated approximately 10% of the time effectively provides therapeutic benefits for both epilepsy and depression [17–19]. These parameters have been shown in both animals and humans to modulate firing rates in brainstem nuclei including the NTS and LC through modulation of several neurotransmitters, one of which is NE, and through modulation of cerebral blood flow [2,20–22].

More recently, high-frequency, burst-patterned stimulation has been explored as an alternative treatment for epilepsy. Imaging studies after stimulation with burst-pattern parameters in primates have shown strong modulation of deep brain targets, particularly in the thalamus [23]. Further, preclinical epilepsy studies in rodents and dogs have suggested that microbursting VNS parameters may provide greater therapeutic benefit than lower 20–30 Hz frequencies [24,25], though potential mechanisms driving these differences have not yet been investigated.

In the current study, we attempted to determine optimal stimulation parameters for PD by altering VNS paradigms using an investigational VNS device (LivaNova Model 1000C, not approved for commercial use) in a double lesion rat model of PD. This model was chosen to mirror the hypothesis of clinical progression put forth by Braak and colleagues that PD-associated neurodegeneration originates in lower brainstem regions, such as the LC, and the degeneration progresses to higher midbrain regions (ie. the SN), then to the cerebrum resulting in the PD-associated motor deficits [8]. Our model consists of using DSP-4 (N-Ethyl-N-(2-chloroethyl)-2-bromobenzylamine hydrochloride) to create an LC-NE lesion, followed by instrastriatal 6-OHDA (6-hydroxydopamine), to create a nigrostriatal lesion [26]. DSP-4 readily crosses the blood brain barrier and has long-lasting effects on LC terminals as early as 5 days post-injection [27,28]. The intrastriatal 6-OHDA creates a slow nigrostriatal lesion due to the retrograde transport of the toxin from striatum to SN-DA cell bodies [29]. The use of this double lesion model has been shown by our group and others to better mimic the behavioral and pathological changes associated with PD, including motor deficits, a loss of SN-DA and LC-NE tyrosine hydroxylase (TH)-positive cells, increased α-synuclein expression, reduced BDNF expression, and increased neuroinflammation [10,26,30]. We hypothesized for the current study that biomimetic, high-frequency VNS more closely resembling LC neuronal properties, would be ideal for upregulating the LC-NE system, consequentially reducing neuroinflammation and motor deficits. Lower frequencies that provide benefits for systemic inflammatory disorders [15,31] were expected to reduce inflammation without improving motor function. We compared these paradigms to current clinical VNS parameters used to treat epilepsy and depression.

Materials and methods

Animals

Adult male Long Evans rats (225 g at start of experiment, Charles River) were used for all studies. Rats were housed in an AAALAC-accredited facility at the Medical University of South Carolina (MUSC), kept at 20–22 °C on a 12 h light:dark cycle. Food (LabDiet 5V75) and water were provided ad libitum. All experiments were approved by the MUSC Institutional Animal Care and Use Committee. Rats were divided into the following groups: control, lesion, lesion + low frequency VNS (lowVNS), lesion + high frequency VNS (stdVNS), and lesion + microburst biomimetic VNS (burstVNS, n = 5 for each group).

Surgical procedures

The same double lesion PD model was utilized for these studies as previously implemented by our group (Fig. 1A) [10,30]. Lesion rats received DSP-4 (50 mg/kg, i.p., Sigma) followed 7 days later by intrastriatal 6-OHDA (6 μg/μL, 2 μL/site, made with 0.02% ascorbate, Sigma) at the following coordinates: Hole 1: AP:+1.6, ML:±2.4, DV: -4.2; Hole 2: AP:+0.2, ML:±3.7, DV: -5.0 [32]. Control rats received an injection of sterile saline (0.9% sodium chloride, 3.1 mL/kg, i.p., Hospira) followed by intrastriatal sterile saline at the same dose and coordinates. VNS therapy systems (LivaNova) were implanted while rats remained under anesthesia (Fig. 1B) [33]. The left vagus nerve and carotid artery were exposed, and bipolar helical leads were coiled around the nerve/artery bundle and sutured to neck muscles. The leads' terminal pin was tunneled subcutaneously to a transverse back incision and connected to the pulse generator. The generator was inserted into a polyester mesh pouch (Ethicon) that was sutured to the underlying back muscle with excess lead length coiled around the pouch. After suturing incisions, connectivity of the implant to the nerve was confirmed using the programming wand and computer (LivaNova). Rats not receiving VNS were instrumented as well, but leads were connected to a weight-matched sham generator instead of the pulse generator.

Treatment

Eleven days post-6-OHDA, rats underwent the assigned VNS paradigm for 10 days (Fig. 1). All VNS rats received continuously cyclic stimulation at 0.75 mA based on previous findings that similar current provided therapeutic effects in this model [10]. Additional VNS details are in Fig. 1C. The system was routinely interrogated to assess the generator battery and lead continuity, showing that all animals received the planned amount of therapeutic stimulation for the duration of the project.

Locomotor activity

Locomotor activity (total distance traveled) was assessed each treatment day in the afternoon during VNS for 30 min using Digiscan (Omnitech) photobeam chambers as previously described [10,34]. Beam breaks were recorded in 5-min bins and reported in cm traveled per 30-min session. Analysis of locomotor data was completed by an individual blinded to treatment groups.

Cylinder task

On the final treatment day, the cylinder task was used to assess forelimb akinesia. Briefly, rats were placed in a plexiglass cylinder and allowed to explore the cylinder for 90 s while being recorded [35]. Cylinder data was analyzed by an individual blinded to treatment groups.

Brain preparation

Immediately following the locomotor session on treatment day 10, rats were anesthetized with isoflurane and decapitated. Brains were removed, and the right prefrontal cortex (PFC) was dissected and frozen at −80 °C for detection of NE. The remaining brain was fixed in 4% paraformaldehyde for 48 h, followed by 30% sucrose for 48 h minimum. Brains were embedded in OCT (Tissue-Tek), frozen, and sectioned at 45 μm through the left striatum, bilateral SN and

LC on a cryostat (Microm). Sections were stored in 0.1 M phosphate buffer before staining.

Norepinephrine Enzyme-Linked Immunosorbent Assay (NE ELISA)

Frozen (−80 °C) right PFC samples were used to assess the concentration of NE in a major LC target region using an ELISA (Abnova). Samples were homogenized using lysis buffer containing protease inhibitor (Calbiochem). Serially diluted standards (0–32 ng of NE) and samples were loaded in duplicate on a pre-coated 96-well plate. Remaining steps were performed according to manufacturer's instructions. The plate was read at 450 nm on a VersaMax plate reader (Molecular Devices). Duplicate values were averaged to obtain a mean NE concentration per animal.

Immunohistochemistry

Immunohistochemical staining was conducted on serial sections from the left striatum (every 12th) and bilateral LC (every 3rd) [10,30] to detect catecholamines using anti-TH (tyrosine hydroxylase, Pelfreez, 1:1000). Inflammation in the SN was assessed via serial sections (every 6th) to detect GFAP (glial fibrillary acidic protein stained astrocytes, Dako, 1:2000) and Iba-1 (ionized calcium-binding adaptor molecule-1 stained microglia, Wako, 1:1000). Briefly, using 4–6 sections per animal, endogenous peroxidases were blocked, tissue permeability was enhanced using sodium meta periodate. Non-specific binding was prevented using 10% normal goat serum for 1 h. Sections were then incubated overnight in primary antibodies. The following day, sections were rinsed, then incubated for 1 h in biotinylated goat anti-rabbit secondary antibody (Vector, 1:200). After rinsing, staining sensitivity was enhanced using avidin-biotin complex (ABC kit, Vector) for 1 h then developed using VIP (Vector). Stained tissue was mounted on gelatin-coated glass slides, dehydrated, and coverslipped using Permount (Fisher).

Immunofluorescent staining

Immunofluorescent staining was used to assess dopaminergic neurons by detecting TH (Abcam, 1:1000) and intracellular α-synuclein (Cell Signaling, 1:250) on 4–6 serial sections through the SN (every 6th) [10,30]. Sections were rinsed in phosphate-buffered saline, then blocked in normal donkey serum (10%) before incubating overnight in primary antibodies. The next day, sections were rinsed, incubated in secondary antibodies for 1 h (TRITC-conjugated donkey anti-sheep, 1:50, FITC-conjugated donkey anti-rabbit, 1:200, Jackson), and rinsed again. Tissue was mounted on gelatin-coated glass slides and coverslipped using FluoroGold.

Semiquantitation of staining density

All immunohistochemical and immunofluorescent analyses (density and counts) were performed by individuals blinded to treatment conditions.

Mean density measures of TH-immunoreactivity (ir) in the dorsal striatum, GFAP-ir in the SN, and Iba-1-ir in the SN were conducted [10,30]. 16-bit images were taken of 4–6 sections per animal using a QImage R3 camera system (QImaging), and mean density measurements were obtained via ImageJ software (NIH) on a scale of 0(white)-65535(black) using a template outline for each region. Background measures were taken for each section and subtracted from the mean density measurement, and these corrected numbers were averaged to obtain mean density per animal.

Intrasomal α-synuclein-ir was assessed using Fluoview software on an Olympus BX-61 confocal microscope (Olympus) keeping acquisition settings consistent across images [10,30]. Z-stack images were analyzed by identifying 45 TH-positive neurons in the TRITC channel from 4 to 6 sections per animal. Using ImageJ's ROI manager function, these same neurons were identified in the FITC channel. Mean fluorescence from α-synuclein was measured in each neuron, then corrected for background fluorescence and averaged per animal.

Stereological cell counting

Quantitative estimates of TH-positive neurons were conducted in the LC along the lateral edge of the fourth ventricle. In the SN, TH-positive neurons included only those in the SN pars compacta. These estimates were calculated using an unbiased optical fractionator live-capture method with StereoInvestigator software (MicroBrightfield) on a BX-61 microscrope (Olympus) fitted with an automated headstage [10,30]. A 10x objective was used to outline the LC (every 3rd) and the SN (every 6th) in a rostral to caudal manner through each region. A systematic random sampling of dissector frames (100 × 100 μm) was used to count neurons using a 20x objective from 4 to 6 sections per animal. StereoInvestigator then extrapolated an estimated population of TH-positive neurons per animal.

Statistical analysis

Graphs were assembled in GraphPad Prism (GraphPad Software). Locomotor activity was analyzed blindly using repeated measures 6 (Treatment) x 10 (Day) analysis of variance (ANOVA) in GraphPad Prism. All other data were analyzed blindly using one-way ANOVA in SPSS (IBM). No datasets violated normal distribution or homogeneity of variance assumptions. Group-wise difference determination was conducted for all ANOVAs using two-sided Tukey's honest significant difference tests at a significance threshold of $p < 0.05$, and corrected significance levels have been reported. Effect sizes for significant one-way ANOVAs and group-wise comparisons have been reported using η^2 and Cohen's d (d), respectively.

Results

Treatment effects on motor behavior

In analyzing daily locomotor activity (Fig. 2A), a repeated measure 6 (Treatment) x 10 (Day) ANOVA showed a significant effect of Treatment ($F(4,20) = 22.42$, $p < 0.0001$, $\eta^2 = 0.8176$) with a significant interaction between Treatment x Day ($F(36,180) = 5.539$, $p < 0.0001$, $\eta^2 = 0.4714$). Upon examining the interaction via Tukey's test, locomotor activity of lesion rats decreased over time ($p < 0.05$), activity of lowVNS rats remained consistent across the 10 treatment days, and activity of stdVNS and burstVNS rats increased over time ($p < 0.05$). When assessing effects of different VNS paradigms on locomotion, lowVNS did not have a significant impact; however, rats receiving higher frequencies of VNS had greater locomotor activity compared to both untreated lesion rats (stdVNS: $p < 0.01$, $d = 5.011$; burstVNS: $p < 0.001$, $d = 4.270$) and lowVNS rats (stdVNS: $p < 0.05$, $d = 2.628$, burstVNS: $p < 0.01$, $d = 2.778$).

Forelimb akinesia was assessed on the last treatment day (Fig. 2B). Using one-way ANOVA to analyze these data, a significant Treatment effect existed ($F(4,20) = 21.69$, $p < 0.0001$, $\eta^2 = 0.8127$). Tukey's test indicated lesion rats reared less than controls ($p < 0.0001$, $d = 7.205$). VNS rats displayed greater rearing time compared to lesion with trends toward more rearing at higher frequencies (lowVNS: $p < 0.05$, $d = 2.825$; stdVNS: $p < 0.001$,

$d = 4.973$; burstVNS: $p < 0.0001$, $d = 2.89$), with only burstVNS rats having similar rearing time to controls.

Treatment effects on the LC-NE system

TH-positive neurons in the LC were counted to evaluate the ability of VNS to attenuate loss in this region (Fig. 3F). One-way ANOVA revealed a significant effect of Treatment on this population ($F(4,20) = 30.29$, $p < 0.0001$, $\eta^2 = 0.8583$). As demonstrated previously [10], lesion rats had significantly fewer LC TH-positive cells than controls (Tukey's, $p < 0.0001$, $d = 5.097$, Fig. 3A–B). All VNS paradigms had greater LC TH-positive neurons over untreated lesion rats (lowVNS: $p < 0.001$, $d = 3.600$; stdVNS: $p < 0.0001$, $d = 4.997$; burstVNS: $p < 0.0001$, $d = 6.698$; Fig. 3C–E). BurstVNS had greater TH-positive neurons compared to lowVNS ($p < 0.01$, $d = 3.108$, Fig. 3C,E) and stdVNS ($p < 0.05$, $d = 2.453$, Fig. 3D–E), with similar numbers to healthy controls (Fig. 3A,E), thereby suggesting that burstVNS provides the greatest attenuation of LC-NE loss.

When assessing NE concentration in PFC, one-way ANOVA showed a significant effect of Treatment ($F(4,20) = 12.35$, $p < 0.0001$, $\eta^2 = 0.7118$, Fig. 3G). Following Tukey's correction, lesion rats had significantly less NE than controls ($p < 0.0001$, $d = 3.446$). All treatment groups had higher NE compared to lesions (lowVNS: $p < 0.05$, $d = 2.582$; stdVNS: $p < 0.01$, $d = 3.177$; burstVNS: $p < 0.001$, $d = 4.115$), with no significant differences between treatment groups. These data demonstrate that VNS effectively attenuates reduction of NE by stimulating the LC-NE system.

Treatment effects on the SN-DA system

Effects of VNS on nigrostriatal DA system degeneration were examined via TH immunohistochemistry and immunofluorescence (Fig. 4A-J,P-Q). One-way ANOVA revealed a Treatment effect in both the striatum ($F(4,20) = 41.41$, $p < 0.0001$, $\eta^2 = 0.8923$) and SN ($F(4,20) = 59.34$, $p < 0.0001$, $\eta^2 = 0.9223$). Tukey's test showed that lesion rats had significantly lower striatal TH-ir and fewer SN TH-positive neurons compared to controls ($p < 0.0001$, striatum: $d = 6.735$, SN: $d = 8.001$, Fig. 4A-B,F-G). While all treatment groups had significantly greater striatal TH-ir (lowVNS: $p < 0.01$, $d = 3.838$; stdVNS: $p < 0.001$, $d = 3.944$; burstVNS: $p < 0.0001$, $d = 5.414$; Fig. 4B–E) and SN TH-positive neurons (lowVNS: $p < 0.05$, $d = 3.298$; stdVNS: $p < 0.0001$, $d = 5.090$; burstVNS: $p < 0.0001$, $d = 7.161$; Fig. 4G–J) compared to untreated lesion animals, the burstVNS paradigm resulted in the greatest beneficial effects on the nigrostriatal DA system (striatum: lowVNS: $p < 0.05$, $d = 2.573$, Fig. 4C,E; SN: lowVNS: $p < 0.0001$, $d = 4.861$, stdVNS: $p < 0.01$, $d = 2.398$, Fig. 4H–J).

As previously shown, intrasomal α-synuclein-ir was higher in lesion rats compared to controls ($p < 0.0001$, $d = 4.570$, Fig. 4K-L) [10]. One-way ANOVA indicated an overall Treatment effect ($F(4,20) = 23.59$, $p < 0.0001$, $\eta^2 = 0.8251$), such that intrasomal α-synuclein-ir was lower for stdVNS ($p < 0.0001$, $d = 3.413$, Fig. 4L,N) and burstVNS ($p < 0.0001$, $d = 4.573$, Fig. 4L,O) treatments. BurstVNS had the lowest α-synuclein-ir compared to lowVNS ($p < 0.01$, $d = 3.271$, Fig. 4M,O), making burstVNS comparable to controls (Fig. 4K,O). These data combined with results from nigrostriatal TH demonstrate that burstVNS provides the greatest benefit for the SN-DA system.

VNS effects on inflammatory markers

While assessing the effects of VNS on neuroinflammation (Fig. 5), a significant effect of Treatment on GFAP (astrocyte marker) and Iba-1 (microglia marker) density existed following one-way ANOVA ($F(4,20) = 31.72$, $p < 0.0001$, $\eta^2 = 0.8638$; $F(4,20) = 28.05$, $p < 0.0001$, $\eta^2 = 0.8487$, respectively). Using Tukey's test, lesion rats had greater GFAP-ir and Iba-1-ir than controls ($p < 0.0001$, GFAP: $d = 7.608$, Iba-1: $d = 5.444$, Fig. 5A-B,F-G). Microglial and astrocyte density were lower in all treatment groups compared to lesion alone ($p < 0.01$; lowVNS: GFAP: $d = 2.083$, Iba-1: $d = 2.714$; stdVNS: GFAP: $d = 4.649$, Iba-1: $d = 3.025$; burstVNS: GFAP: $d = 4.633$, Iba-1: $d = 4.144$; Fig. 5B-E,G-J). However, burstVNS was the only treatment with comparable GFAP-ir and Iba-1-ir to controls (Fig. 5A,E-F,J) and had significantly lower GFAP-ir compared to lowVNS rats ($p < 0.05$, $d = 1.796$, Fig. 5C,E). These

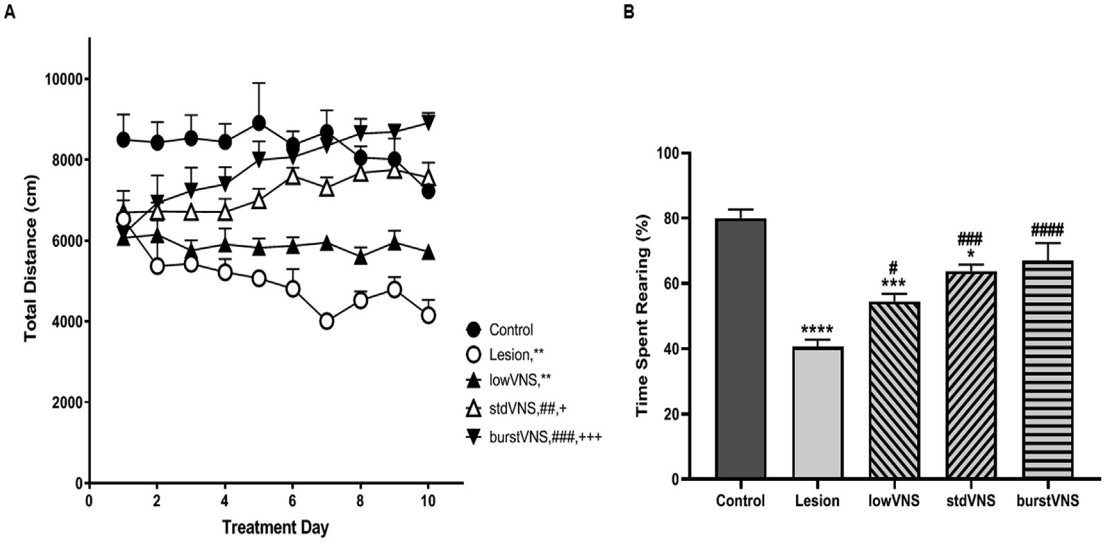

Fig. 2. Higher VNS frequencies provided greater behavioral improvement than low frequencies. (A) Total distance traveled for each group (measured in cm) across all 10 stimulation days shows decreased locomotor activity in untreated lesion rats over the 10 days, while locomotor activity of stdVNS and burstVNS rats improved. Significance marked in figure legend denotes statistical differences on day 10. (B) Time spent rearing during the cylinder task to assess forelimb akinesia on treatment day 10 shows decreased rearing in untreated lesion rats. All VNS groups had increased rearing with trends toward greater rearing at higher VNS frequencies. (*$p < 0.05$, **$p < 0.01$, ***$p < 0.001$, ****$p < 0.0001$; post hoc comparisons: * to Control, # to Lesion, + to lowVNS).

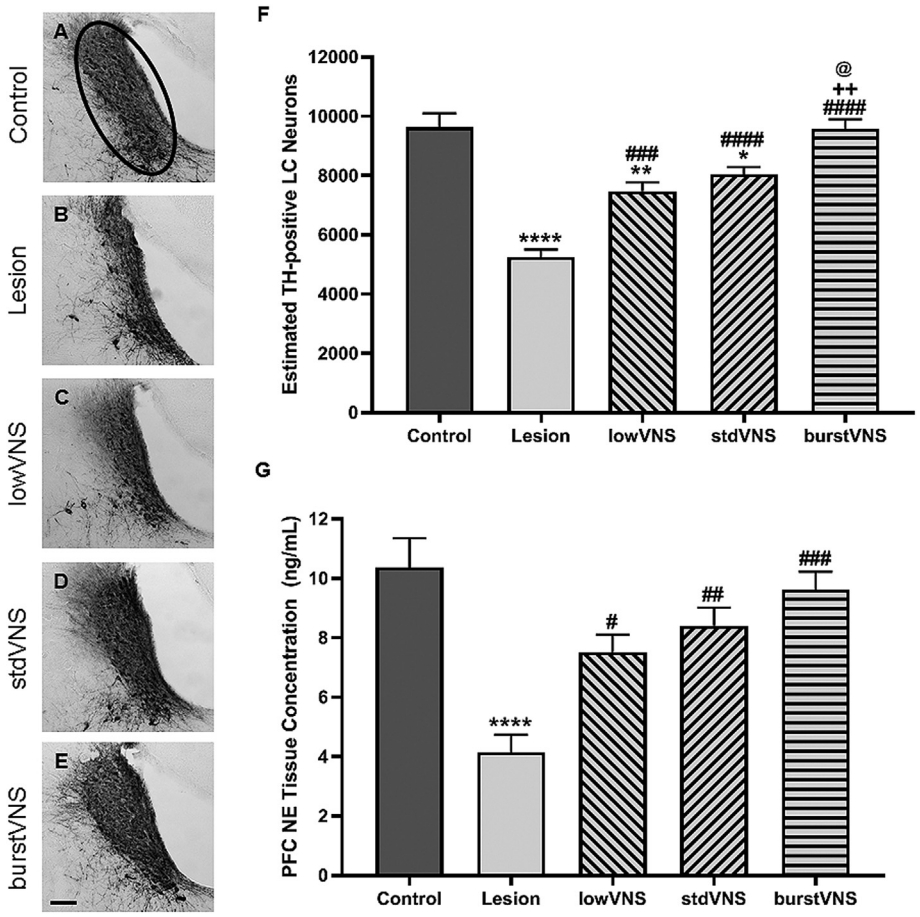

Fig. 3. VNS attenuated loss of TH-positive neurons in LC and yielded elevated NE in LC targets compared to untreated lesion rats. The outlined measurement area for TH-positive cell counts in LC is shown in A, with representative photomicrographs shown for TH-positive LC neurons from each treatment group in A-E (scale = 100 μm). Untreated lesion rats had fewer LC TH-positive cells than controls (A,B), and VNS slightly attenuated this loss for lowVNS (C) and stdVNS (D) groups. BurstVNS provided the most extensive attenuation of TH-positive cell loss in the LC (E). Estimated TH-positive cell counts are quantified in F. NE tissue concentration in prefrontal cortex (PFC) determined by ELISA is quantified in G, demonstrating that while lesion rats had decreased NE compared to control rats, VNS resulted in higher NE for all 3 treatment groups. (*$p < 0.05$, **$p < 0.01$, ***$p < 0.001$, ****$p < 0.0001$; post hoc comparisons: * to Control, # to Lesion, + to lowVNS, @ to stdVNS).

data show that while all VNS paradigms displayed reduced inflammatory markers, burstVNS has the greatest overall anti-inflammatory effect.

Discussion

The focus of this study was to determine the most effective VNS paradigm in a PD model by examining degenerating neural pathways and behaviors associated with PD. While the efficacy of VNS in this model was previously assessed [10], the current study expanded those findings by comparing three unique VNS paradigms. Overall, results from this study demonstrated that VNS, regardless of paradigm, results in reduced inflammation, attenuated LC and SN phenotypic neuronal loss, and enhanced motor function. However, higher stimulation frequencies were more effective for most of these measures in this model. Particularly, burstVNS showed the greatest treatment potential.

A double lesion model of PD was used for these studies to mimic the ascending pattern of degeneration in humans with progression from the LC to the SN, before resulting in motor deficits [8,36]. We have previously shown that at this timepoint in lesion development, motor deficits and LC-NE and SN-DA phenotypic loss occur with no difference in the number of total cells present; therefore, the timepoint used for our studies is prior to neuronal death [10,30]. In this lesion model we also saw higher intrasomal α-synuclein, demonstrating a pathological expression pattern similar to PD [37,38] that may contribute to greater neuroinflammation [39], whereas non-pathological α-synuclein is localized to neuronal processes and is thought to assist in neurotransmitter release [40]. While current pharmacological therapies for PD help manage symptoms [41,42], these therapies cannot delay symptom progression [43,44]. Because of these issues, a large portion of PD research has been devoted to development of disease-modifying therapies.

The vagus nerve has previously been implicated in PD progression [8,45]. Some groups have focused on interrupting propagation of α-synuclein from the gut to the brain via vagotomy to slow the disease [9]. Alternatively, our group took a different approach by stimulating the vagus nerve to increase NE output and reduce mechanisms of neurodegeneration, as shown for other preclinical models [1,2,15,31]. We previously showed that VNS delivered twice daily attenuated PD-like pathology and behavior [10]. Another preclinical PD study in rats demonstrated that transcutaneous auricular VNS alleviated neuroinflammation, resulting in reduced SN-DA phenotypic loss and greater motor function, possibly through nicotinic acetylcholine receptor activation [46]. Small human pilot studies in PD showed that a single session of transcutaneous VNS can improve gait [47,48], highlighting the

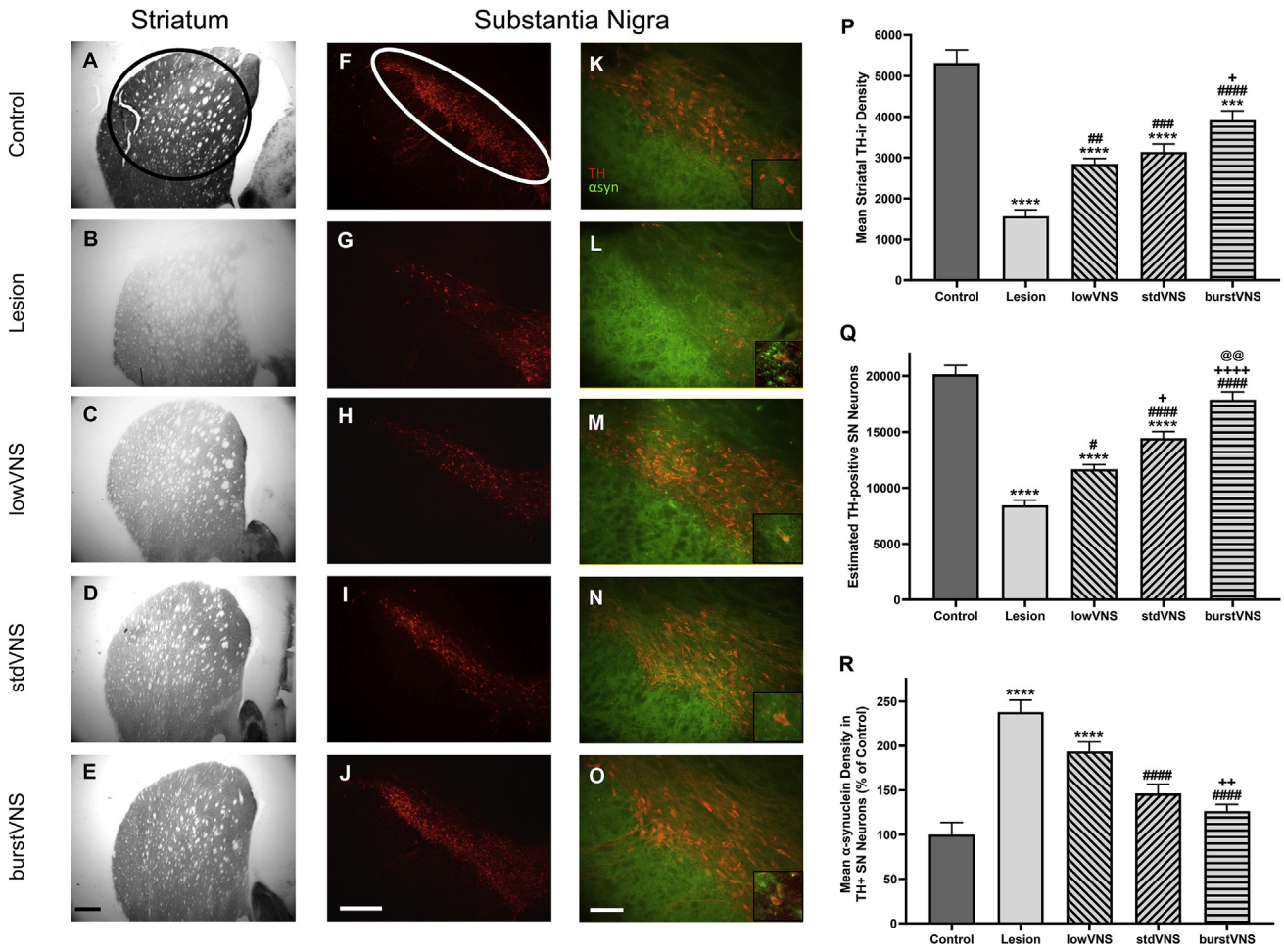

Fig. 4. All VNS treatment groups had attenuated loss of striatal TH-ir and SN TH-positive neurons, and burstVNS provided the greatest reduction in intrasomal α-synuclein. Representative photomicrographs show TH-positive striatal fibers (A-E, scale = 500 μm, measurement outline shown in A), TH-positive SN neurons (F-J, scale = 250 μm, measurement outline shown in F), SN TH-positive neurons (red) overlaid with α-synuclein (green) from each treatment group (K–O, scale = 100 μm, insets show localization of α-synuclein in TH-positive neurons). Lesion rats had lower striatal TH-ir (A,B) and fewer TH-positive cells in the SN (F,G) compared to control rats. VNS resulted in attenuation of striatal TH-ir and TH-positive cell loss in SN (C-E, H-J), with the greatest attenuation in the burstVNS group (E,J). Further, in the SN, lesion rats had increased instrasomal α-synuclein within remaining TH-positive cells (K,L). While lowVNS had no significant effect on α-synuclein (M), higher VNS frequencies resulted in lower intrasomal α-synuclein for both stdVNS (N) and burstVNS (O) rats. Quantifications: striatal TH-ir density shown in P, TH-positive cells in SN shown in Q, and SN intrasomal α-synuclein density shown in R. (*$p < 0.05$, **$p < 0.01$, ***$p < 0.001$, ****$p < 0.0001$; post hoc comparisons: * to Control, # to Lesion, + to lowVNS, @ to stdVNS). (For interpretation of the references to colour in this figure legend, the reader is referred to the Web version of this article.)

therapeutic potential of VNS. However, implantable systems were chosen here to increase mobility for motor assessment during daily VNS. For this current study, three distinct, clinically-relevant VNS paradigms were utilized in the same PD model used previously to determine ideal parameters for stimulation. The stdVNS frequency and duration reflected settings used to treat epilepsy and depression clinically [49,50], and lowVNS settings delivered daily for only a short time previously reduced peripheral inflammation in rodents and clinical trials for rheumatoid arthritis [31,51,52]. While burstVNS has not been extensively investigated, preclinical epilepsy studies suggested microburst VNS may be more effective than standard paradigms delivering regular pulses [24,25].

Since low-frequency VNS (10 Hz) has been shown to decrease peripheral inflammation [15,31], we examined its effectiveness on neuroinflammation. Although lowVNS resulted in lower neuroinflammation and provided slight benefits for SN-DA neurons and behavior, these effects were not as extensive as effects of the other two VNS paradigms. Therefore, lowVNS was not suitable for maximal benefit in this disease model, similar to its effects on depression [49]. Alternatively, the frequency used for stdVNS (20 Hz) delivered at similar duration has previously increased NE release in PFC [20,21] and cerebral blood flow [22,53], and induced desynchronization of electroencephalogram rhythms [54,55] to provide anti-convulsive effects for epilepsy. In this study, stdVNS reduced neuroinflammation, attenuated LC-NE and SN-DA TH-positive cell loss, and improved behavior to a greater extent than lowVNS. These findings reflect previous preclinical rodent studies that showed 20 Hz VNS reduces neuroinflammation to protect against cerebral ischemia [56,57]. VNS effects are typically attributed to activation of myelinated efferent and afferent vagal A fibers [58]. The 10 Hz used for lowVNS is traditionally thought to more closely target vagal efferents, whereas the 20 Hz used for stdVNS is thought to better activate the NTS and higher brain regions, although the precise mechanism of action remains unknown.

PD-like pathology and behavior were most attenuated in the current study by burstVNS. Previous reports suggest that microburst VNS may provide greater benefit over standard VNS in a partial epilepsy rodent model via prevention of seizure threshold decline [24] and in dogs where greater changes in cerebral blood flow occurred [25]. Several microburst VNS paradigms also

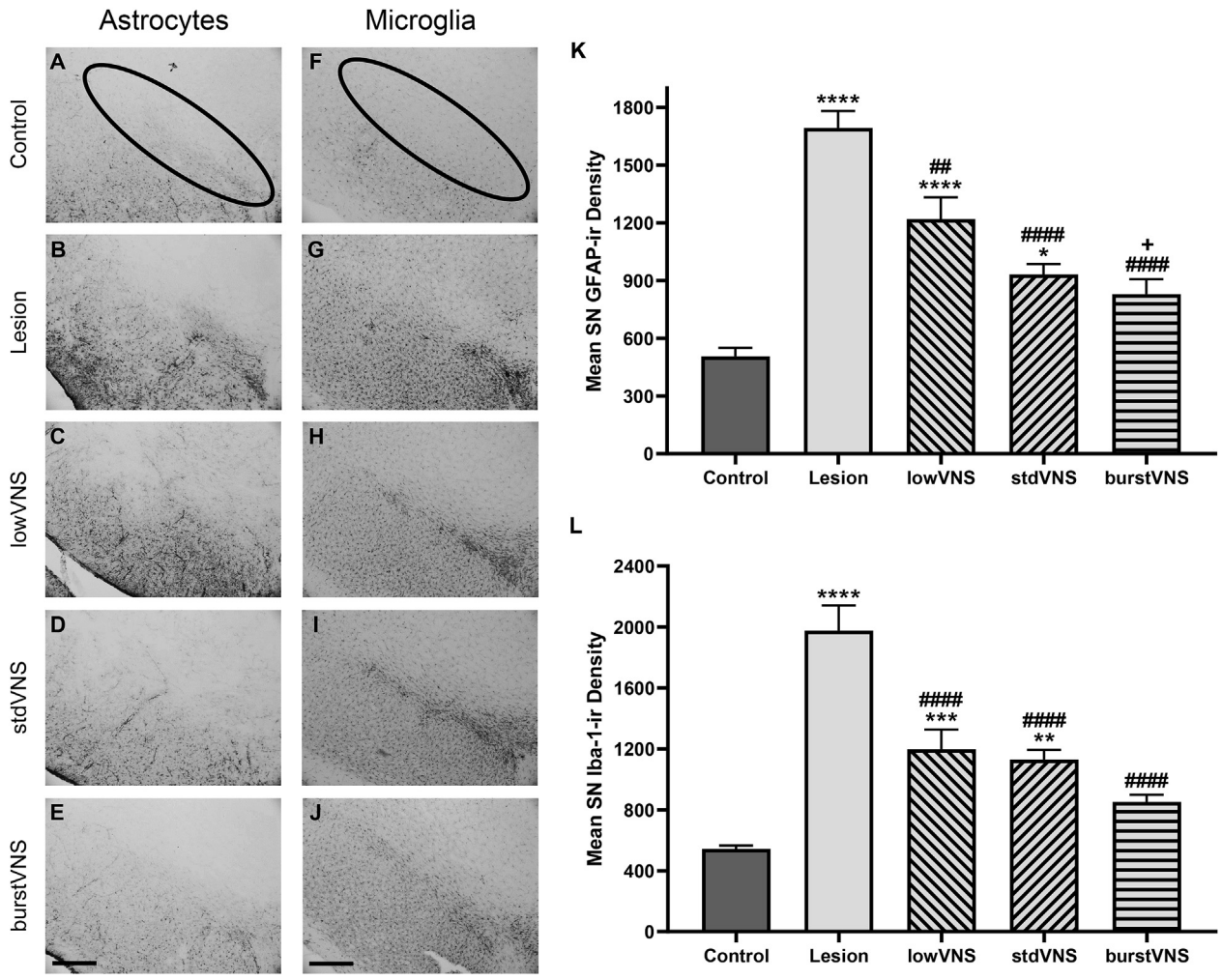

Fig. 5. All VNS treatment groups displayed lower glial density in SN. Representative photomicrographs from SN show representative glial staining from each treatment group for astrocytes (GFAP, A-E, scale = 250 μm, measurement outline shown in A) and microglia (Iba-1, F-J, scale = 250 μm, measurement outline shown in F). Untreated lesion rats had greater glial density compared to control rats for both astrocytes (A,B) and microglia (F,G). VNS resulted in lower glial density for lowVNS (C,H), stdVNS (D,I), and burstVNS (E,J), with only burstVNS having comparable glial density to control rats. Mean density is quantified for astrocytes in K and for microglia in L. (*$p < 0.05$, **$p < 0.01$, ***$p < 0.001$, ****$p < 0.0001$; post hoc comparisons: * to Control, # to Lesion, + to lowVNS).

provided therapeutic benefits in a primate model of epilepsy without inducing transient bradycardia which has been observed during standard VNS [23]. Intermittent theta burst stimulation (a type of transcranial magnetic stimulation administered at higher frequencies in shorter bursting intervals compared to conventional repetitive transcranial magnetic stimulation protocols) was previously shown to be more tolerable with enhanced cortical excitability, further suggesting bursting stimulation paradigms are more beneficial than conventional paradigms [59–61]. We hypothesize that burstVNS had the greatest effect in our study because the frequent stimulation bursts in intermittent patterns reflect natural rhythms of LC activation [62], elevating evoked potentials in higher brain regions [63]. Norepinephrine also enhances astrocytic supportive functions, enhances microglial neurotrophic factor production, and suppresses microglial pro-inflammatory molecule production, processes thought to be mediated by activation of glial noradrenergic receptors [64,65]. Therefore, more effective activation of LC-NE neurons induced by bursting VNS may lead to greater reduction of neuroinflammation in LC target regions (ie SN), a hypothesis for future investigation. These findings combined with our study demonstrate that burstVNS provides the highest therapeutic value for PD compared to the alternative paradigms tested.

The effects of VNS on neuroinflammation in this PD model showed that VNS was able to modify mechanisms of degeneration to attenuate TH-positive loss in addition to alleviating motor symptoms. While in rodents these results happened on the order of days to weeks [5,10,66], it is important to note that in epilepsy and depression patients, VNS effects occurred over longer periods on the order of months to years [67–70]. Therefore, while initial pilot studies using external VNS suggested promising motor benefits for PD [47,48], a similar timecourse should be expected for long-term VNS treatment in PD patients due to chronic, ongoing degeneration. While other anti-inflammatory strategies such as non-steroidal anti-inflammatory drugs have failed to yield convincing clinical results for PD [71], VNS provides greater benefit by altering multiple mechanisms of degeneration. Previous studies showed that in addition to inhibiting neuroinflammation, VNS reduced oxidative stress [52,72] and increased neurotrophic factor signaling [4,73]. Through modification of these mechanisms, intrasomal α-syncuclein may be reduced [39,74] and SN-DA and LC-NE phenotypic loss may be attenuated [10,75], leading to reduction of motor deficits. Thus, the multi-modal function of VNS may effectively slow PD disease progression where strategies focusing on a single mechanism at a time have failed.

Conclusions

Overall, we can conclude that VNS provides great therapeutic potential for PD in a minimally invasive manner. In our PD model, VNS resulted in improved motor function, attenuated loss of TH-positive neurons in LC and SN, and lowered neuroinflammation and intrasomal α-synuclein in SN. For these reasons, VNS may effectively slow disease progression by targeting mechanisms of degeneration rather than focusing on symptom management alone, thereby providing a large advantage over currently prescribed therapies. Our data also indicate that higher stimulation frequencies, specifically microburst VNS, had the greatest impact on markers of PD progression and should be evaluated in future translational research.

CRediT authorship contribution statement

Ariana Q. Farrand: Project administration, Investigation, Data curation, Formal analysis, Visualization, Writing - original draft, Writing - review & editing. **Ryan S. Verner:** Conceptualization, Methodology, Software, Funding acquisition, Project administration, Data curation, Writing - review & editing. **Ryan M. McGuire:** Conceptualization, Methodology, Software, Funding acquisition, Project administration, Data curation, Writing - review & editing. **Kristi L. Helke:** Project administration, Methodology, Investigation, Writing - review & editing. **Vanessa K. Hinson:** Conceptualization, Funding acquisition, Writing - review & editing. **Heather A. Boger:** Conceptualization, Methodology, Funding acquisition, Project administration, Investigation, Data curation, Formal analysis, Visualization, Supervision, Writing - original draft, Writing - review & editing.

Declaration of competing interest

RV and RM are employed by LivaNova, PLC and hold stock options. HB received funding from LivaNova, PLC to independently conduct this study. VH has received consulting fees from LivaNova, PLC.

Acknowledgements

The authors would like to sincerely thank Luis Aponte-Cofresí and Duncan Nowling for their assistance with immunohistochemistry for these studies. We would also like to thank Rebecca Gregory for help with tissue processing.

This work was supported by a pilot grant from the MUSC Barmore Fund (HAB and VKH) and by LivaNova, PLC in Houston, TX. All study design, data collection, analysis, writing, and submission decisions were conducted by the authors of this manuscript, not by funding sources.

References

[1] Follesa P, Biggio F, Gorini G, Caria S, Talani G, Dazzi L, et al. Vagus nerve stimulation increases norepinephrine concentration and the gene expression of BDNF and bFGF in the rat brain. Brain Res 2007;1179:28–34.
[2] Dorr AE, Debonnel G. Effect of vagus nerve stimulation on serotonergic and noradrenergic transmission. J Pharmacol Exp Therapeut 2006;318(2):890–8.
[3] Tononi G, Cirelli C. Sleep function and synaptic homeostasis. Sleep Med Rev 2006;10(1):49–62.
[4] Biggio F, Gorini G, Utzeri C, Olla P, Marrosu F, Mocchetti I, et al. Chronic vagus nerve stimulation induces neuronal plasticity in the rat hippocampus. Int J Neuropsychopharmacol 2009;12(9):1209–21.
[5] Furmaga H, Shah A, Frazer A. Serotonergic and noradrenergic pathways are required for the anxiolytic-like and antidepressant-like behavioral effects of repeated vagal nerve stimulation in rats. Biol Psychiatr 2011;70(10):937–45.
[6] Tofaris GK, Buckley NJ. Convergent molecular defects underpin diverse neurodegenerative diseases. J Neurol Neurosurg Psychiatry 2018;89(9):962–9.
[7] Worth PF. When the going gets tough: how to select patients with Parkinson's disease for advanced therapies. Practical Neurol 2013;13(3):140–52.
[8] Braak H, Rub U, Gai WP, Del Tredici K. Idiopathic Parkinson's disease: possible routes by which vulnerable neuronal types may be subject to neuroinvasion by an unknown pathogen. J Neural Transm (Vienna) 2003;110(5):517–36.
[9] Svensson E, Horváth-Puhó E, Thomsen RW, Djurhuus JC, Pedersen L, Borghammer P, et al. Vagotomy and subsequent risk of Parkinson's disease. Ann Neurol 2015;78(4):522–9.
[10] Farrand AQ, Helke KL, Gregory RA, Gooz M, Hinson VK, Boger HA. Vagus nerve stimulation improves locomotion and neuronal populations in a model of Parkinson's disease. Brain Stimul 2017;10(6):1045–54.
[11] Johnson RL, Wilson CG. A review of vagus nerve stimulation as a therapeutic intervention. J Inflamm Res 2018;11:203–13.
[12] Bonaz B, Sinniger V, Pellissier S. Vagus nerve stimulation: a new promising therapeutic tool in inflammatory bowel disease. J Intern Med 2017;282(1):46–63.
[13] Koopman FA, van Maanen MA, Vervoordeldonk MJ, Tak PP. Balancing the autonomic nervous system to reduce inflammation in rheumatoid arthritis. J Intern Med 2017;282(1):64–75.
[14] Lu KH, Cao J, Oleson S, Ward MP, Phillips RJ, Powley TL, et al. Vagus nerve stimulation promotes gastric emptying by increasing pyloric opening measured with magnetic resonance imaging. Neuro Gastroenterol Motil 2018;30(10):e13380.
[15] Koopman FA, Chavan SS, Miljko S, Grazio S, Sokolovic S, Schuurman PR, et al. Vagus nerve stimulation inhibits cytokine production and attenuates disease severity in rheumatoid arthritis. Proc Natl Acad Sci U S A 2016;113(29):8284–9.
[16] Tang MW, Koopman FA, Visscher JP, de Hair MJ, Gerlag DM, Tak PP. Hormone, metabolic peptide, and nutrient levels in the earliest phases of rheumatoid arthritis-contribution of free fatty acids to an increased cardiovascular risk during very early disease. Clin Rheumatol 2017;36(2):269–78.
[17] Rush AJ, Sackeim HA, Marangell LB, George MS, Brannan SK, Davis SM, et al. Effects of 12 months of vagus nerve stimulation in treatment-resistant depression: a naturalistic study. Biol Psychiatr 2005;58(5):355–63.
[18] Sackeim HA, Brannan SK, Rush AJ, George MS, Marangell LB, Allen J. Durability of antidepressant response to vagus nerve stimulation (VNS). Int J Neuropsychopharmacol 2007;10(6):817–26.
[19] Yamamoto T. Vagus nerve stimulation therapy: indications, programing, and outcomes. Neurol Med -Chir 2015;55(5):407–15.
[20] Hassert DL, Miyashita T, Williams CL. The effects of peripheral vagal nerve stimulation at a memory-modulating intensity on norepinephrine output in the basolateral amygdala. Behav Neurosci 2004;118(1):79–88.
[21] Roosevelt RW, Smith DC, Clough RW, Jensen RA, Browning RA. Increased extracellular concentrations of norepinephrine in cortex and hippocampus following vagus nerve stimulation in the rat. Brain Res 2006;1119(1):124–32.
[22] Vonck K, De Herdt V, Bosman T, Dedeurwaerdere S, Van Laere K, Boon P. Thalamic and limbic involvement in the mechanism of action of vagus nerve stimulation, a SPECT study. Seizure 2008;17(8):699–706.
[23] Szabó C, Salinas FS, Papanastassiou AM, Begnaud J, Ravan M, Eggleston KS, et al. High-frequency burst vagal nerve simulation therapy in a natural primate model of genetic generalized epilepsy. Epilepsy Res 2017;138:46–52.
[24] Alexander GM, McNamara JO. Vagus nerve stimulation elevates seizure threshold in the kindling model. Epilepsia 2012;53(11):2043–52.
[25] Martlé V, Peremans K, Raedt R, Vermeire S, Vonck K, Boon P, et al. Regional brain perfusion changes during standard and microburst vagus nerve stimulation in dogs. Epilepsy Res 2014;108(4):616–22.
[26] Ledreux A, Boger HA, Hinson VK, Cantwell K, Granholm AC. BDNF levels are increased by aminoindan and rasagiline in a double lesion model of Parkinson's disease. Brain Res 2016;1631:34–45.
[27] Fritschy JM, Geffard M, Grzanna R. The response of noradrenergic axons to systemically administered DSP-4 in the rat: an immunohistochemical study using antibodies to noradrenaline and dopamine-beta-hydroxylase. J Chem Neuroanat 1990;3(4):309–21.
[28] Ranson RN, Gaunt K, Santer RM, Watson AH. The effects of ageing and of DSP-4 administration on the micturition characteristics of male Wistar rats. Brain Res 2003;988(1–2):130–8.
[29] Fischer DL, Kemp CJ, Cole-Strauss A, Polinski NK, Paumier KL, Lipton JW, et al. Subthalamic nucleus deep brain stimulation employs trkB signaling for neuroprotection and functional restoration. J Neurosci 2017;37(28):6786–96.
[30] Farrand AQ, Helke KL, Aponte-Cofresí L, Gooz MB, Gregory RA, Hinson VK, et al. Effects of vagus nerve stimulation are mediated in part by TrkB in a Parkinson's disease model. Behav Brain Res 2019;373:112080.
[31] Meregnani J, Clarençon D, Vivier M, Peinnequin A, Mouret C, Sinniger V, et al. Anti-inflammatory effect of vagus nerve stimulation in a rat model of inflammatory bowel disease. Auton Neurosci 2011;160(1–2):82–9.
[32] Paxinos G, Watson C. The rat brain in stereotaxic coordinates. second ed. San Diego, CA: Academic Press; 1986.
[33] Phillips Campbell RB, Duffourc MM, Schoborg RV, Xu Y, Liu X, KenKnight BH, et al. Aberrant fecal flora observed in Guinea pigs with pressure overload is mitigated in animals receiving vagus nerve stimulation therapy. Am J Physiol Gastrointest Liver Physiol 2016;311(4):G754–62.

[34] Boger HA, Middaugh LD, Huang P, Zaman V, Smith AC, Hoffer BJ, et al. A partial GDNF depletion leads to earlier age-related deterioration of motor function and tyrosine hydroxylase expression in the substantia nigra. Exp Neurol 2006;202(2):336–47.
[35] Nobile CW, Palmateer JM, Kane J, Hurn PD, Schallert T, Adkins DL. Impaired limb reaction to displacement of center of gravity in rats with unilateral striatal ischemic injury. Transl Stroke Res 2014;5(5):562–8.
[36] Srinivasan J, Schmidt WJ. Behavioral and neurochemical effects of noradrenergic depletions with N-(2-chloroethyl)-N-ethyl-2-bromobenzylamine in 6-hydroxydopamine-induced rat model of Parkinson's disease. Behav Brain Res 2004;151(1–2):191–9.
[37] Bendor JT, Logan TP, Edwards RH. The function of α-synuclein. Neuron 2013;79(6):1044–66.
[38] Huang L, Deng M, He Y, Lu S, Liu S, Fang Y. beta-asarone increases MEF2D and TH levels and reduces alpha-synuclein level in 6-OHDA-induced rats via regulating the HSP70/MAPK/MEF2D/Beclin-1 pathway: chaperone-mediated autophagy activation, macroautophagy inhibition and HSP70 up-expression. Behav Brain Res 2016;313:370–9.
[39] Zhang QS, Heng Y, Yuan YH, Chen NH. Pathological alpha-synuclein exacerbates the progression of Parkinson's disease through microglial activation. Toxicol Lett 2017;265:30–7.
[40] Shimozawa A, Fujita Y, Kondo H, Takimoto Y, Terada M, Sanagi M, et al. Effect of L-DOPA/benserazide on propagation of pathological α-synuclein. Front Neurosci 2019;13:595.
[41] Robottom BJ. Efficacy, safety, and patient preference of monoamine oxidase B inhibitors in the treatment of Parkinson's disease. Patient Prefer Adherence 2011;5:57–64.
[42] Kalia LV, Lang AE. Parkinson's disease. Lancet 2015;386(9996):896–912.
[43] Dorszewska J, Prendecki M, Lianeri M, Kozubski W. Molecular effects of L-dopa therapy in Parkinson's disease. Curr Genom 2014;15(1):11–7.
[44] Li SY, Wang YL, Liu WW, Lyu DJ, Wang F, Mao CJ, et al. Long-term levodopa treatment accelerates the circadian rhythm dysfunction in a 6-hydroxydopamine rat model of Parkinson's disease. Chin Med J (Engl) 2017;130(9):1085–92.
[45] Kim S, Kwon SH, Kam TI, Panicker N, Karuppagounder SS, Lee S, et al. Transneuronal propagation of pathologic α-synuclein from the gut to the brain models Parkinson's disease. Neuron 2019;103(4):627–41. e7.
[46] Jiang Y, Cao Z, Ma H, Wang G, Wang X, Wang Z, et al. Auricular vagus nerve stimulation exerts antiinflammatory effects and immune regulatory function in a 6-OHDA model of Parkinson's disease. Neurochem Res 2018;43(11):2155–64.
[47] Mondal B, Choudhury S, Simon B, Baker MR, Kumar H. Noninvasive vagus nerve stimulation improves gait and reduces freezing of gait in Parkinson's disease. Mov Disord 2019;34(6):917–8.
[48] Morris R, Yarnall AJ, Hunter H, Taylor JP, Baker MR, Rochester L. Noninvasive vagus nerve stimulation to target gait impairment in Parkinson's disease. Mov Disord 2019;34(6):918–9.
[49] Müller HH, Kornhuber J, Maler JM, Sperling W. The effects of stimulation parameters on clinical outcomes in patients with vagus nerve stimulation implants with major depression. J ECT 2013;29(3):e40–2.
[50] Giordano F, Zicca A, Barba C, Guerrini R, Genitori L. Vagus nerve stimulation: surgical technique of implantation and revision and related morbidity. Epilepsia 2017;58(Suppl 1):85–90.
[51] Clarençon D, Pellissier S, Sinniger V, Kibleur A, Hoffman D, Vercueil L, et al. Long term effects of low frequency (10 hz) vagus nerve stimulation on EEG and heart rate variability in Crohn's disease: a case report. Brain Stimul 2014;7(6):914–6.
[52] Yi C, Zhang C, Hu X, Li Y, Jiang H, Xu W, et al. Vagus nerve stimulation attenuates myocardial ischemia/reperfusion injury by inhibiting the expression of interleukin-17A. Exp Ther Med 2016;11(1):171–6.
[53] Henry TR, Bakay RA, Pennell PB, Epstein CM, Votaw JR. Brain blood-flow alterations induced by therapeutic vagus nerve stimulation in partial epilepsy: II. prolonged effects at high and low levels of stimulation. Epilepsia 2004;45(9):1064–70.
[54] Koo B. EEG changes with vagus nerve stimulation. J Clin Neurophysiol 2001;18(5):434–41.
[55] Boon P, Vonck K, van Rijckevorsel K, El Tahry R, Elger CE, Mullatti N, et al. A prospective, multicenter study of cardiac-based seizure detection to activate vagus nerve stimulation. Seizure 2015;32:52–61.
[56] Xiang YX, Wang WX, Xue Z, Zhu L, Wang SB, Sun ZH. Electrical stimulation of the vagus nerve protects against cerebral ischemic injury through an anti-infammatory mechanism. Neural Regen Res 2015;10(4):576–82.
[57] Lu XX, Hong ZQ, Tan Z, Sui MH, Zhuang ZQ, Liu HH, et al. Nicotinic acetylcholine receptor Alpha7 subunit mediates vagus nerve stimulation-induced neuroprotection in acute permanent cerebral ischemia by a7nAchR/JAK2 pathway. Med Sci Mon Int Med J Exp Clin Res 2017;23:6072–81.
[58] McAllen RM, Shafton AD, Bratton BO, Trevaks D, Furness JB. Calibration of thresholds for functional engagement of vagal A, B and C fiber groups. Bioelectron Med (Lond) 2018;1(1):21–7.
[59] Ni Z, Gunraj C, Kailey P, Cash RF, Chen R. Heterosynaptic modulation of motor cortical plasticity in human. J Neurosci 2014;34(21):7314–21.
[60] Han C, Chen Z, Liu L. Commentary: effectiveness of theta burst vs. high-frequency repetitive transcranial magnetic stimulation in patients with depression (THREE-D): a randomized non-inferiority trial. Front Hum Neurosci 2018;12:255.
[61] Dhami P, Knyahnytska Y, Atluri S, Lee J, Courtney DB, Croarkin PE, et al. Feasibility and clinical effects of theta burst stimulation in youth with major depressive disorders: an open-label trial. J Affect Disord 2019;258:66–73.
[62] Miguelez C, Aristieta A, Cenci MA, Ugedo L. The locus coeruleus is directly implicated in L-DOPA-induced dyskinesia in parkinsonian rats: an electrophysiological and behavioural study. PloS One 2011;6(9):e24679.
[63] Ito S, Craig AD. Vagal-evoked activity in the parafascicular nucleus of the primate thalamus. J Neurophysiol 2005;94(4):2976–82.
[64] O'Donnell J, Zeppenfeld D, McConnell E, Pena S, Nedergaard M. Norepinephrine: a neuromodulator that boosts the function of multiple cell types to optimize CNS performance. Neurochem Res 2012;37(11):2496–512.
[65] Jiang L, Chen SH, Chu CH, Wang SJ, Oyarzabal E, Wilson B, et al. A novel role of microglial NADPH oxidase in mediating extra-synaptic function of norepinephrine in regulating brain immune homeostasis. Glia 2015;63(6):1057–72.
[66] Hays SA, Khodaparast N, Ruiz A, Sloan AM, Hulsey DR, Rennaker RL, et al. The timing and amount of vagus nerve stimulation during rehabilitative training affect poststroke recovery of forelimb strength. Neuroreport 2014;25(9):676–82.
[67] Handforth A, DeGiorgio CM, Schachter SC, Uthman BM, Naritoku DK, Tecoma ES, et al. Vagus nerve stimulation for partial-onset seizures: a randomized active-control trial. Neurology 1998;51(1):48–55.
[68] Nahas Z, Marangell LB, Husain MM, Rush AJ, Sackeim HA, Lisanby SH, et al. Two-year outcome of vagus nerve stimulation (VNS) for treatment of major depressive episodes. J Clin Psychiatr 2005;66(9):1097–104.
[69] Bajbouj M, Merkl A, Schlaepfer TE, Frick C, Zobel A, Maier W, et al. Two-year outcome of vagus nerve stimulation in treatment-resistant depression. J Clin Psychopharmacol 2010;30(3):273–81.
[70] Elliot RE, Morsi A, Tanweer O, Grobelny B, Geller E, Carlson C, et al. Efficacy of vagus nerve stimulation over time: review of 65 consecutive patients with treatment-resistant epilepsy treated with VNS > 10 years. Epilepsy Behav 2011;20(3):478–83.
[71] Samii A, Etminan M, Wiens MO, Jafari S. NSAID use and the risk of Parkinson's disease: systematic review and meta-analysis of observational studies. Drugs Aging 2009;26(9):769–79.
[72] Chen X, He X, Luo S, Feng Y, Liang F, Shi T, et al. Vagus nerve stimulation attenuates cerebral microinfarct and colitis-induced cerebral microinfarct aggravation in mice. Front Neurol 2018;9:798.
[73] Carreno FR, Frazer A. Activation of signaling pathways downstream of the brain-derived neurotrophic factor receptor, TrkB, in the rat brain by vagal nerve stimulation and antidepressant drugs. Int J Neuropsychopharmacol 2014;17(2):247–58.
[74] Tan SH, Karri V, Tay NWR, Chang KH, Ah HY, Ng PQ, et al. Emerging pathways to neurodegeneration: dissecting the critical molecular mechanisms in Alzheimer's disease, Parkinson's disease. Biomed Pharmacother 2019;111:765–77.
[75] Hwang O. Role of oxidative stress in Parkinson's disease. Exp Neurobiol 2013;22(1):11–7.
[76] Shiramatsu TI, Hitsuyu R, Ibayashi K, Kanzaki R, Kawai K, Takahashi H. Effect of vagus nerve stimulation on neural adaptation in thalamo-cortical system in rats. Conf Proc IEEE Eng Med Biol Soc 2016;2016:1834–7.